MAGNETIC RESONANCE IN CHEMISTRY
Magn. Reson. Chem. 2007; **45**: 929–936
Published online 18 September 2007 in Wiley InterScience
(www.interscience.wiley.com) DOI: 10.1002/mrc.2072

MRC

Dynamic NMR study and theoretical calculations on the conformational exchange of valsartan and related compounds

Fang Li,[1,3] Huiting Zhang,[1,3] Ling Jiang,[1]* Weinong Zhang,[1] Jing Nie,[2] Yuqi Feng,[2] Minghui Yang[1] and Maili Liu[1]*

[1] Wuhan Center for Magnetic Resonance, State Key Laboratory of Magnetic Resonance and Atomic and Molecular Physics, Wuhan Institute of Physics and Mathematics, Chinese Academy of Sciences, Wuhan, 430071, People's Republic of China
[2] Department of Chemistry, Wuhan University, Wuhan, 430072, People's Republic of China
[3] Graduate School, Chinese Academy of Sciences, Beijing 100049, People's Republic of China

Received 21 June 2007; Revised 26 July 2007; Accepted 31 July 2007

Valsartan (1), an antihypertensive drug of the sartan family, and three related compounds, 3-methyl-2-((2′-(1-methyl-1H-tetrazol-5-yl)biphenyl-4-ylmethyl) pentanoylamino)butyric acid (2), 3-isopropyl-6-propyl-4-(2′-(1H-tetrazol-5-yl)biphenyl-4-ylmethyl) morpholine-2,5-dione (3), and 3-isopropyl-6-propyl-4-(4′-(1H-tetrazol-5-yl)biphenyl4-ylmethyl) morpholine-2,5-dione (4), were studied by nuclear magnetic resonance (NMR) spectroscopy. Assignment of ^{1}H and ^{13}C NMR resonances for the compounds were completed using COSY, HSQC and HMBC techniques. It was found that each of the compounds 1, 2, and 4 had two sets of ^{1}H and ^{13}C resonances, suggesting the presence of two conformers in solution. Based on NOESY experiments at different temperatures, thermodynamic parameters of the conformational exchange process were deduced for these compounds. The exchange barrier was found to be 17.9 ± 0.7, 18.5 ± 0.8, and 17.7 ± 0.6 kcal mol^{-1} with the corresponding free energy difference (ΔG) of 0.32 ± 0.04, 0.23 ± 0.01, and 0.13 ± 0.04 kcal mol^{-1} for 1, 2, and 4, respectively, at 298 K. Two conformations of valsartan were elucidated by NMR spectroscopy and quantum chemistry calculation. The results showed that two conformers of valsartan interchange via rotation about the C(O)–N bond. Copyright © 2007 John Wiley & Sons, Ltd.

KEYWORDS: NMR; valsartan; exchange rate; conformational analysis; quantum chemistry calculation

INTRODUCTION

Valsartan (**1**), (S)-*N*-valeryl-*N*-((2′-(1*H*-tetrazol-5-yl)-biphenyl-4-yl) methyl) valine, is an antihypertensive drug belonging to a series of sartan agents, which are well known to act as angiotensin II receptor antagonists.[1] One of the common ways of treatment of hypertension is to prevent the progression of target organ damage by controlling blood pressure, as stated in guidelines recently published in the sixth report of the Joint National Committee on prevention, detection, evaluation, and treatment of high blood pressure.[2,3] The angiotensin II receptor antagonists are highly affective antihypertensive agents with excellent tolerability profiles.[4] They selectively block the angiotension type 1 (AT1) receptor that is responsible for vasoconstriction, prevent salt and water retention, but have no effect on the angiotensin type 2 (AT2) that is thought to have cardioprotective and inhibitory effects on growth.[5] A number of analytical methods have been used for quantitative determination of valsartan in biological samples,[6–10] and their protein-binding characteristics have also been investigated in different animal species and tissues.[11–13] However, the conformational properties of valsartan still remains unknown. Since the structural features of some sartan drugs are helpful in understanding their dynamic properties in membrane bilayers and docking to AT1 receptor,[14–17] it is of great interest to perform a conformational analysis of valsartan, which would not only give some insights into its biological activity, but help in developing drugs with better biological profile.

NMR spectroscopy, in particular the 2D NMR technique, has proved to be a standard tool for studying molecular structure, conformations and dynamics in solution.[18–20] In a recent study, we reported[21] isolation of three impurities in crude valsartan and one of them was identified as 3-methyl-2-((2′-(1-methyl-1*H*-tetrazol-5-yl)biphenyl-4-ylmethyl)pentanoylamino) butyric acid (**2**). The other two were identified as 3-isopropyl-6-propyl-4-(2′-(1*H*-tetrazol-5-yl)biphenyl-4-ylmethyl) morpholine-2,5-dione (**3**), and 3-isopropyl-6-propyl-4-(4′-(1*H*-tetrazol-5-yl)biphenyl-4-ylmethyl) morpholine-2,5-dione (**4**). It has been noticed that there are two distinct rotational isomers at wide range of temperature for compound **1**. In the present work, we studied the

*Correspondence to: Ling Jiang and Maili Liu, Wuhan Center for Magnetic Resonance, State Key Laboratory of Magnetic Resonance and Atomic and Molecular Physics, Wuhan Institute of Physics and Mathematics, Chinese Academy of Sciences, Wuhan, 430071, People's Republic of China. E-mail: lingjiang@wipm.ac.cn; ml.liu@wipm.ac.cn

MRC

structural properties of valsartan (**1**) and three related compounds or byproducts (**2, 3, 4**) by using multidimensional NMR spectroscopy, and found that each of the compounds **1**, **2,** and **4** had two conformers that were in slow exchange on the NMR time scale in CD_3OD solvent. We used NMR approach to establish the thermodynamic and kinetic parameters involved in the exchange process between conformers of compounds **1**, **2,** and **4**, and in combination with structural simulation based on density functional theory (DFT), the spatial structures of valsartan two conformers were elucidated.

EXPERIMENTAL

Samples

Raw valsartan was supplied by a Pharmaceutical Company of China and purified by high performance liquid chromatography with a SPD-10A UV-visible detector. Three hundred milligrams of the sample was dissolved in 10 ml acetonitrile-water (80/20, v/v), and 1 ml was chromatographed on Hyspersil ODS2 (250 × 10.0 mm, 5 μm), eluting with 0.2% acetic acid (v/v in H_2O)-acetonitrile (40/60, v/v) at a flow rate of 5 ml/min, to give retention time of 14 ∼ 18 min for valsartan and 22 ∼ 28 min for fraction I. Fraction I was collected and evaporated to dryness, dissolved in acetonitrile-water (80/20, v/v), then chromatographed on ZORBAX SB-CN (250 mm × 4.6 mm, 5 μm) with 0.2% acetic acid (v/v in H_2O)-acetonitrile (45/55, v/v) to afford fraction II and fraction III. Fraction II was subjected to Hyspersil ODS2 column eluted with 0.2% acetic acid (v/v in H_2O)-acetonitrile (40/60, v/v) by the rate of 5 ml/min to yield compound **2**. Fraction III was subjected to Hyspersil ODS2 column eluted with 0.2% acetic acid (v/v in H_2O)-acetonitrile (38/62, v/v) by the rate of 5 ml/min to obtain compounds **3** and **4**. Electrospray ionization mass spectra of these compounds were measured with a PE-SCIEX mass spectrometer.

NMR measurements

All NMR experiments were carried out on a Varian INOVA-500 machine with ^1H and ^{13}C frequencies of 500.12 and 125.03 MHz, respectively. 1D and 2D NMR spectra of the compounds were measured in 0.5 ml of CD_3OD at 298 K. Chemical shifts were given on the δ scale and were calibrated to the residual solvent signal of methanol at δ 3.30 for ^1H and δ 49.3 for ^{13}C. Single pulse ^1H NMR spectra were acquired using conventional method with a spectral width of 5.8 kHz, 256 scans and 32 K data points. Proton decoupled ^{13}C NMR spectra were obtained conventionally with spectral width of 26 kHz, 20 K scans and 32 K data points. $^1H-^1H$ correlation spectra (COSY and TOCSY) were acquired into a 512(F1) × 2048 (F2) time-domain data matrix with 16 scans per t_1 increment and a spectral width of 5 kHz in both F_1 and F_2 dimensions. The mixing time for magnetization transfer was 100 ms for the TOCSY experiment. One-bond $^1H-^{13}C$ single-quantum correlation (HSQC) spectra were recorded with 64 scans per t_1 increment covering the spectral width of 20 and 4.5 kHz in the F_1 (^{13}C) and F_2 (^1H) dimensions, respectively. The time-domain matrix was 400 (F_1) by 2048 (F_2) and the frequency-domain matrix was 1024 (F_1) by 2048 (F_2) after zero-filling in the F_1 dimension. The interpulse delay was set to 3.57 ms focusing on an average J_{CH} value of 140 Hz. Long-range $^1H-^{13}C$ multiple-quantum correlation (HMBC) spectra had very similar parameters as those used in the HSQC experiments, while the delay was set to 62.5 ms [equals $J_{CH} = 8$ Hz], 125 ms [equals $J_{CH} = 4$ Hz] and 250 ms [equals $J_{CH} = 2$ Hz]. NOESY spectra were acquired with a mixing time of 0.3 s, data matrix 2 K × 2 K (512 increments to 2 K zero-filling in F_1, 2 K in F_2), 32 transients in each increment, spectral width 4.5 kHz. Spin-lattice relaxation times were measured using conventional inversion-recovery method. Residual solvent signal was suppressed using presaturation approach.

Computational details

Structure calculation of valsartan was conducted using Amber8[22] for molecular dynamics (MD) simulation and Gaussian03[23] for quantum chemical calculation. Initial structures were generated from random conformations and refined by a short time MD simulation and a following energy minimization. The one with the lowest energy was chosen as the starting structure used in the following three-step systematic searching of five dihedral angles carried out in vacuum. In each step of the systematic searching, energy surface was built for the molecule with all the coordinates relaxed except the target dihedral angle. The coordinates of the minimum on the energy surface was then taken as the starting structure for the next step of systematic searching. Semi-empirical PM3 method was applied during the first and the second step with a stepsize of 5° and 10°, respectively. DFT with B3LYP/6-31G* and enlarged basis set 6-311G** were employed in the third step to obtain more accurate results, with the scanning intervals of 30°.

RESULTS AND DISCUSSIONS

NMR signal assignment of compounds 1–4

Assignments of ^1H and ^{13}C NMR resonances for the compounds **1**–**4** were achieved conventionally from integral inspection and chemical shifts of the ^1H and ^{13}C NMR spectra, from the observed through-bond connection in the 2D COSY and TOCSY spectra, observed through-space proton correlations in the 2D NOESY spectra (Fig. 1(a)), and from $^{13}C,^1H$ correlations based 2D NMR spectra (HSQC, HMBC). The unambiguous ^{13}C and ^1H chemical shift assignments of **1**–**4** in CD_3OD solution at 298 K are shown in Table 1.

The structure of valsartan, which was assigned unequivocally to simplify the assignments of compounds **2**, **3,** and **4**, is given in Scheme 1. The MS spectrum of **1** exhibited a series of product ions, m/z 434 ($[M-H]^-$), 350 ($[(M-85]^-$), 304 ($[350-46]^-$), 235 ($[304-69]^-$), 192($[235-43]^-$), which are attributed to the sequential loss of proton → *n*-pentanal → formic acid → isobutyronitrile → hydrazoic acid present in the molecule. And the fragment pattern was similar to that of losartan.[24] The vital ion, which was produced by cleavage on the bond of the acyl nitrogen and the bridging methylene group, is at m/z 235, $[CH_2(C_{12}H_8)(CN_4H)]$.

Compound **2** was obtained as pale yellow crystals. Electrospray ionization mass spectrometry(ESI-MS) showed

DOI: 10.1002/mrc

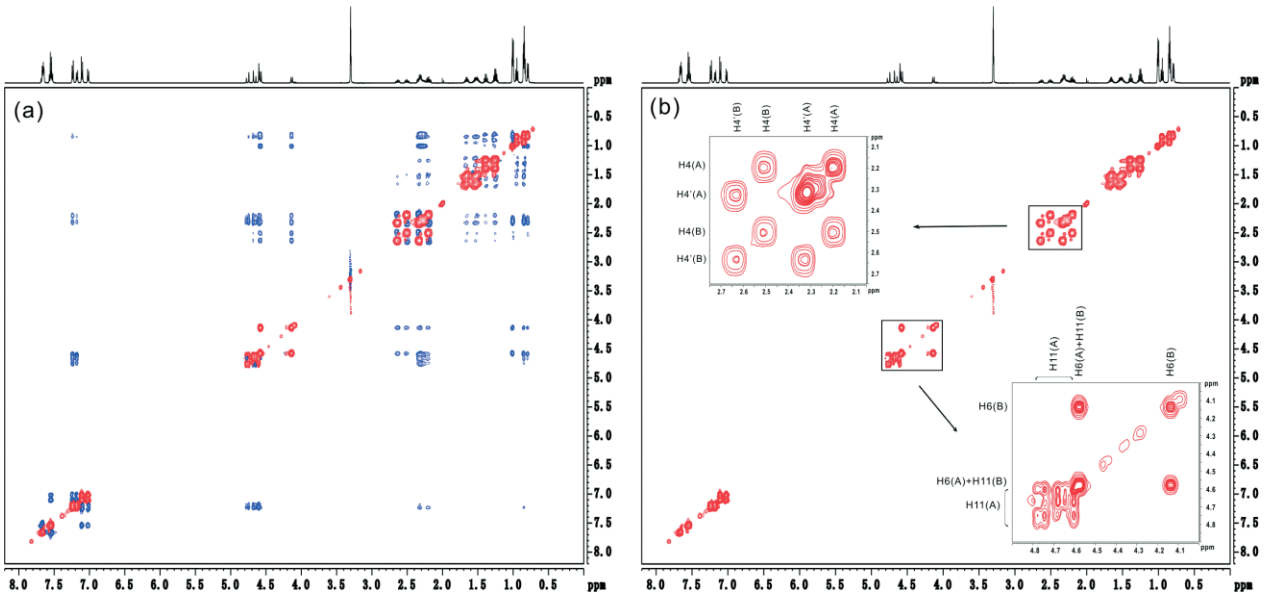

Figure 1. 2D NOESY spectra of valsartan (**1**) in CD_3OD at 298 K recorded on a Varian Inova-500 spectrometer with a mixing time of 300 ms. (a) NOESY spectrum showing both negative (blue) and positive (red) peaks. (b) NOESY spectrum only showing the exchanging peaks of the two conformers. Sample exchanging peaks were expanded and labeled according to the atom nomenclature described in Scheme 1.

a molecular ion peak at m/z 448 ($[M-H]^-$), consistent with a molecular formula $C_{25}H_{31}N_5O_3$, which was also confirmed by its ^1H and ^{13}C NMR spectra data. The MS spectrum of **2** exhibited a series of product ions, m/z 364 ($[M-85]^-$), 318 ($[364-46]^-$), 249 ($[318-69]^-$), 235 ($[249-14]^-$), 206 ($[249-43]^-$), 192 ($[235-14]^-$), which indicated that compound **2** had a similar structure with valsartan. The product ions of **2** at m/z 235 and 249 suggested a methyl had replaced the hydrogen on the tetrazole ring rather than the one on the carboxyl, which was confirmed by the simultaneous existence of product ions at m/z 192 and 206. Moreover, the ^1H NMR spectrum of compound **2** gave essentially the same characteristics as those found in **1**, except an extra singlet at δ 3.36, which was observed to have a correlation with C-24 at δ 156.8 in the 2D HMBC spectrum. NOEs between the proton at δ 3.36 and H-17, H-16, H-22 in NOESY spectrum suggested a methyl substitution on the position shown in Scheme 1 (**2**).

Compound **3** was acquired as white powder. ESI-MS showed a quasi-molecular ion peak at m/z 432 ($[M-H]^-$), compatible with a molecular formula $C_{24}H_{27}N_5O_3$, in agreement with the ^1H and ^{13}C NMR spectral data. The MS spectrum of **3** gave a series of product ions, m/z 404 ($[M-28]^-$), 360 ($[404-44]^-$), 332 ($[360-28]^-$), 304 ($[(332-28]^-$), 276 ($[304-28]^-$), 198 ($[M-235]^-$), 154 ($[198-44]^-$). The key ion, which might have been produced by cleavage on the bond of the acyl nitrogen and the bridging methylene group, is at m/z 198 ($[433-235]^-$) corresponding to $[C_3H_7(C_4H_2O_3N)C_3H_7]$. The major difference observed between ^1H and ^{13}C NMR spectra data for **3** and **1** was the absence of one proton at carbon atom C-4 and the change in the ^{13}C chemical shift of C-4 [δ_C 34.8 (**1**) – 78.7 (**3**), Δ_C = 43.9]. Moreover, in HMBC spectrum, the proton H-4 displayed a long-range correlation with carbon atom C-10. Based on the above results, the structure of **3** was determined as 3-isopropyl-6-propyl-4-[2′-(1*H*-tetrazol-5-yl)biphenyl-4-ylmethyl] morpholine-2,5-dione (Scheme 1).

Compound **4** was also isolated as white powder, which almost had the same ESI-MS as **3** and was consistent with a molecular formula $C_{25}H_{31}N_5O_3$ either. A comparison of the ^1H and ^{13}C NMR data for **4** with those for **3** showed that the signals were in good agreement, except that the signals from phenyl ring had a rather little difference. Analyzing the heteronuclear and homonuclear correlations from 2D NMR spectra, it was revealed that the difference was caused by the para orientation of tetrazole to biphenyl ring in **4**. Hence compound **4** was established as 3-isopropyl-6-propyl-4-[4′-(1*H*-tetrazol-5-yl)biphenyl4-ylmethyl]morpholine-2,5-dione (Scheme 1).

Thermodynamic parameters of exchange process

Analysis of the assignments for compounds **1**, **2,** and **4** showed that some protons gave two sets of sharp and well-resolved resonances, as well as their attached carbon signals, suggesting the presence of two conformers in solution. This hypothesis was further confirmed by the existence of cross peaks between these signals in NOESY spectra, some of which were expanded in Fig. 1(b), illustrating that two conformers were exchanging at a slow exchange rate on the NMR time scale.[25–27]

The dynamic equilibrium of the exchange reaction of two conformers A ↔ B at certain temperature (A refers to the major peak of the pairs at 298 K and B refers to the minor one) can be described by the equilibrium constant $K_{AB} = [B]/[(A]$, which can be easily determined by the concentrations of each conformer in solution using either ^1H NMR or ^{13}C NMR. In this study, ^1H NMR spectra of **1**, **2,** and **4** were recorded at five different temperatures ranging from 293 to 313 K. The distributions of these conformers were estimated by the integrals of the corresponding proton signals. As the

DOI: 10.1002/mrc

Table 1. ^{1}H and ^{13}C NMR chemical shifts (in ppm) for compounds **1**–**4** in CD_3OD solution at 298 K. **1′**, **2′**, and **4′** are exchanging conformers of compounds **1**, **2,** and **4** which have lower signal intensities, respectively

	1		**1′**		**2**		**2′**		**3**		**4**		**4′**	
Number	^{13}C	^{1}H	^{13}C	^{1}H	^{13}C	^{1}H	^{13}C	^{1}H	^{13}C	^{1}H	^{13}C	^{1}H	^{13}C	^{1}H
1	14.5	0.84(*t*, 7.4)	14.5	0.95(*t*, 7.4)	14.5	0.85(*t*, 7.3)	14.5	0.95(*t*, 7.4)	14.4	0.97(*t*, 7.4)	14.1	0.82(*t*, 7.3)	14.2	0.94(*t*, 7.3)
2	23.7	1.24	23.8	1.38	23.7	1.25	23.7	1.38	19.0	1.47	20.7	1.28	20.8	1.38
3	28.8	1.51	28.9	1.66	28.8	1.52	28.9	1.65	34.8	1.89[a], 2.02[b]	38.8	1.77[a], 1.92[b]	38.7	1.88[a], 2.02[b]
4	34.8	2.19[a], 2.33[b]	34.7	2.50[a], 2.64[b]	34.8	2.18[a], 2.34[b]	34.7	2.50[a], 2.64[b]	78.7	5.13	55.9	4.47	55.0	5.03
5	177.5	–	177.3	–	177.4	–	177.2	–	168.5	–	172.7	–	172.9	–
6	65.2	4.58(*d*, 10.1)	68.2	4.14(*d*, 10.7)	65.3	4.57(*d*, 10.3)	68.4	4.12(*d*, 10.3)	66.7	3.91(*d*, 7.1)	68.4	4.08	70.0	4.12
7	29.6	2.31	29.5	2.24	29.5	2.31	29.6	2.26	32.8	2.31	29.8	2.44	29.7	2.29
8	19.7	0.84(*d*, 6.8)	19.6	0.79(*d*, 6.7)	19.7	0.84(*d*, 6.5)	19.6	0.8 (*d*, 6.5)	18.9	1.02(*d*, 6.8)	20.0	0.90(*d*, 6.7)	20.0	0.84(*d*, 6.6)
9	20.9	1.00(*d*, 6.5)	20.3	1.01(*d*, 6.5)	20.9	1.00(*d*, 6.5)	20.3	1.01(*d*, 6.5)	20.5	1.08(*d*, 6.8)	21.8	1.05(*d*, 6.3)	20.6	1.03(*d*, 6.3)
10	173.9	–	173.3	–	173.9	–	173.3	–	168.1	–	172.3	–	171.4	–
11	50.9	4.62[a], 4.80[b]	47.6	4.60	50.7	4.62[a], 4.81[b]	47.5	4.57[a], 4.63[b]	50.3	4.21[a], 5.16[b]	53.3	4.68[a], 4.91[b]	48.1	4.66
12	139.1	–	139.8	–	139.6	–	140.4	–	137.4	–	137.6	–	139.0	–
13	128.1	7.24	129.0	7.18	128.6	7.26	129.4	7.19	129.1	7.21(*d*, 8.0)	128.2	7.33(*d*, 7.8)	128.8	7.1 (*d*, 7.9)
14	130.6	7.10	130.1	7.02	130.3	7.11	129.7	7.01	130.9	7.12(*d*, 8.0)	130.8	7.12(*d*, 7.5)	130.2	7.00(*d*, 7.5)
15	140.0	–	139.1	–	139.7	–	139.0	–	140.5	–	141.4	–	140.0	–
16	130.6	7.10(*d*, 8.3)	130.1	7.02(*d*, 8.3)	130.3	7.11(*d*, 8.3)	129.7	7.01(*d*, 8.3)	130.9	7.12(*d*, 8.0)	130.8	7.12(*d*, 7.5)	130.2	7.00(*d*, 7.5)
17	128.1	7.24(*d*, 8.3)	129.0	7.18(*d*, 8.3)	128.6	7.26(*d*, 8.3)	129.4	7.19(*d*, 8.3)	129.1	7.21(*d*, 8.0)	128.2	7.33(*d*, 7.8)	128.8	7.15(*d*, 7.9)
18	143.4	–	143.6	–	143.4	–	143.6	–	143.1	–	143.2	–	143.5	–
19	132.1	7.55	132.1	7.53	131.8	7.64	131.8	7.65	132.1	7.56	131.8	7.49	128.9	7.49
20	131.9	7.67	132.8	7.66	133.4	7.74	133.4	7.73	131.9	7.66	132.0	7.61	131.7	7.58
21	129.3	7.56	129.2	7.54	129.5	7.60	129.4	7.57	129.2	7.55	127.9	–	128.2	–
22	132.8	7.65	132.0	7.64	132.5	7.61	132.6	7.59	132.7	7.67	132.0	7.61	131.7	7.58
23	124.7	–	124.5	–	123.7	–	123.6	–	124.4	–	131.8	7.49	128.9	7.49
24	156.9	–	157.0	–	156.8	–	157.0	–	157.1	–	159.1	–	159.9	–
–CH3	–	–	–	–	34.6	3.36	34.6	3.31	–	–	–	–	–	

[a,b] Chemical shift of nonequivalent protons of methylenes. Symbols and values in parses correspond to the peak splitting and coupling constant $^{3}J_{HH}$, where *d* represents doublet and *t* represents triplet.

MRC

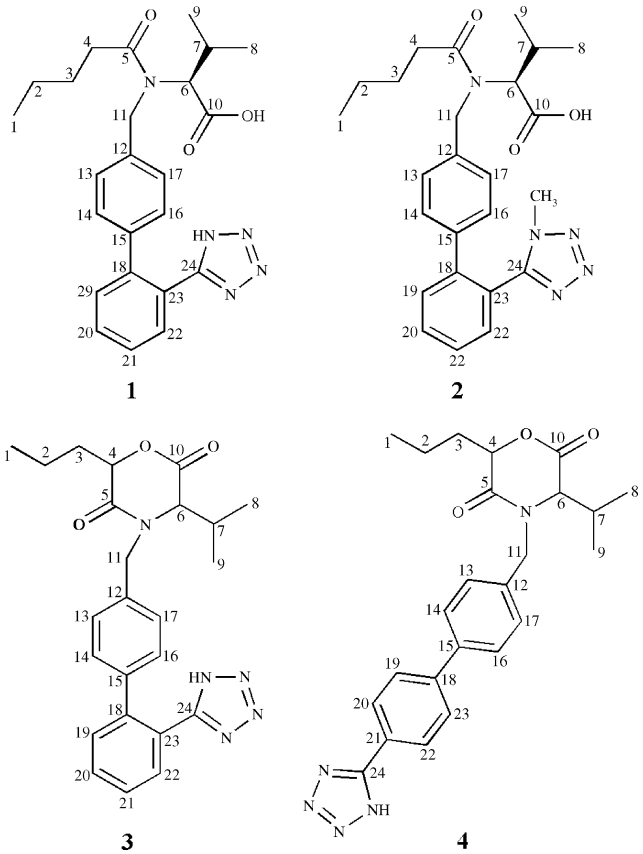

Scheme 1. Chemical structure of compounds **1**–**4**, with all the carbons numbered.

temperature rose, the population of conformer B increased at the expense of conformer A. From the ratios of these integrals, the equilibrium constants for each exchanging proton at variable temperatures were calculated and listed in Table 2.

The equilibrium constant K has a relation to the Gibbs free energy difference ΔG° given by Eqn (1), which is usually broken into its enthalpy ΔH° and entropy ΔS°.

$$\ln K = -\Delta G^\circ/RT = -\Delta H^\circ/RT + \Delta S^\circ/R \qquad (1)$$

In this equation, R is the gas constant and T is the temperature. The results of these thermodynamic parameters of compounds **1**, **2,** and **4** are shown in Table 3. The positive values of Gibbs free energy difference for all three compounds indicated that conformer A was preferred in solution at the temperatures tested in this study, which is consistent with the fact that conformer A gave higher signal intensities in all proton spectra. The small entropy values suggested that the exchange process only contained a simple conformational change in these small molecules.

Table 3. Thermodynamic parameters of exchange process for compounds **1**, **2** and **4** obtained from Eqn (1)

Compound	$\Delta H^\circ \pm$ Std (kcal mol^{-1})	$\Delta S^\circ \pm$ Std (kcal mol$^{-1}\cdot$ s^{-1})	$\Delta G^\circ \pm$ Std (kcal mol^{-1})
1	0.30 ± 0.05	-0.03 ± 0.18	0.32 ± 0.04
2	0.28 ± 0.06	0.19 ± 0.18	0.23 ± 0.01
4	0.72 ± 0.16	1.98 ± 0.48	0.13 ± 0.04

Kinetic parameters of the conformational exchange

The NOESY experiment provides an excellent way to investigate the slow exchange process between sites. An estimation of the exchange rate k can be obtained from the data matrices M and M_0 given by 2D and 1D NMR data based on the well-known relation given below Eqn (2),[28,29] where L is the kinetic matrix containing the exchange rate information and t_m is the mixing time of the NOESY experiment.

$$M = \exp(Lt_m) \bullet M_0 \qquad (2)$$

The solution of Eqn (2) gives k_{AB}, the exchange rate from conformer A to B, and k_{BA} from conformer B to A. Activation enthalpy $\Delta H^\ddagger$ is usually used to evaluate the exchange process which can be obtained by a linear regression of the $ln(k/T)$ and $1/T$ data according to Eqn (3), an Eyring plot.

$$ln(k/T) = -\Delta H^\ddagger/RT + ln(k_b/h) + \Delta S^\ddagger/R \qquad (3)$$

where R, k_b and h are all constants with the values of 8.31451 $J \cdot mol^{-1} \cdot K^{-1}$, $1.381 \cdot 10^{-23}$ $J\,K^{-1}$ and $6.626 \cdot 10^{-34}$ $J \cdot s$, respectively.

For compound **1**, the exchanging protons which gave two sets of peaks at chemical shifts δ 1.24/δ 1.38, δ 1.51/δ 1.66, δ 7.10/δ 7.02 and δ 7.24/δ 7.18 were assigned to be H-2, H-3, H-16 and H-17, respectively. These four protons were chosen because they were relatively less overlapped with other signals to avoid overestimation of the exchange rate. The calculation showed that the exchange rates of these protons are almost the same and increased quickly as temperature increased. Same calculations were done for compounds **2** and **4** at various temperatures and the results were shown in Table 4 as well. Compound **2** had similar exchange rate to compound **1** while the exchange rate of compound **4** was much slower, almost one third of the other two.

Table 2. Equilibrium constants K_{AB} for compounds **1**, **2,** and **4** in CD_3OD at 293–313 K

	1				**2**				**4**			
T(K)	H-2	H-3	H-16	H-17	H-2	H-3	H-16	H-17	H-4	H-7	H-16	H-17
293	0.568	0.581	0.593	0.603	0.668	0.666	0.668	0.699	0.807	0.836	0.710	0.758
298	0.571	0.582	0.600	0.607	0.670	0.673	0.676	0.701	0.834	0.853	0.734	0.802
303	0.576	0.586	0.606	0.613	0.676	0.681	0.683	0.707	0.842	0.863	0.768	0.813
308	0.585	0.589	.0609	0.622	0.678	0.683	0.689	0.710	0.844	0.871	0.782	0.825
313	0.590	0.591	0.611	0.629	0.683	0.698	0.696	0.711	0.858	0.890	0.790	0.840

DOI: 10.1002/mrc

MRC

Table 4. Exchange rates $k_{AB}(s^{-1})$ for protons of compounds **1**, **2,** and **4** in NOESY spectrum recorded at 293–313 K

	1				**2**				**4**			
T(K)	H-2	H-3	H-16	H-17	H-2	H-3	H-16	H-17	H-4	H-7	H-16	H-17
293	0.64	0.60	0.68	0.71	0.63	0.55	0.61	0.68	0.22	0.24	0.24	0.25
298	1.01	0.99	1.12	1.01	1.05	0.97	1.06	1.07	0.35	0.40	0.41	0.40
303	1.73	1.62	1.88	1.94	1.69	1.48	1.70	1.82	0.57	0.64	0.59	0.64
308	2.72	2.50	3.00	3.18	2.68	2.54	2.76	2.61	0.90	1.01	1.02	1.08
313	3.91	3.84	4.50	5.38	3.99	3.95	4.50	4.56	1.65	1.48	1.55	1.69

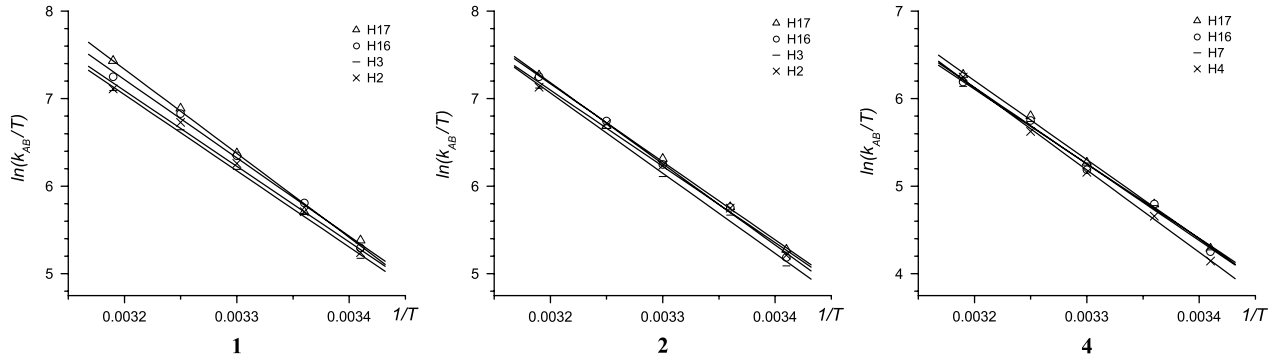

Figure 2. Eyring plots of $ln(k_{AB}/T)$ against $1/T$ used in estimating the exchange barrier for different protons of compounds **1**, **2,** and **4**.

Based on these results, the activation enthalpy $\Delta H^{\ddagger}$ of each compound was estimated as well, which were 17.9 ± 0.7, 18.5 ± 0.8, and 17.7 ± 0.6 kcal mol^{-1}, for compounds **1**, **2,** and **4**, respectively. Figure 2 illustrated the linear-regression fit of the data points which gave r^2 values of greater than 0.99.

Conformational analysis of valsartan

Because the total amount of the byproducts, compound **2**, **3,** and **4**, was very small and they did not show potential biological activities, we only analyzed the conformation of valsartan by using NOESY experiment and quantum chemistry calculation.

NMR results

The NOESY experiment provides structural information through the NOE cross peaks, whose magnitudes are inversely proportional to the sixth power of the interproton distance in space. After carefully checking the cross peaks in the NOESY spectrum of valsartan, we found that, for both conformers, the intensities of the NOEs between protons H-14/H-16 and H-19 did not have much difference, indicating an orientation bias of the two phenyl rings. However, the NOE patterns of the aliphatic part were quite different. The protons H-7, H-8 and H-9 of the isopropyl group have NOE cross peaks to the methylene H-11 and aromatic H-13/H-17 in both conformers. But for the *n*-butyl group, NOE cross peaks from protons H-2, H-3 and H-4 to the methylene H-11 as well as the aromatic H-13/H-17 on the phenyl spacer were observed in conformer A, while they did not exist in conformer B, suggesting different orientation around the peptide bond from N to the attached carbonyl.

Computational analysis

In order to have a clearer picture of the valsartan conformation, structure calculation was carried out using MD simulation and quantum chemical calculation. Several dihedral angles (τ) were defined as following to make the discussion easier:

$$\tau 1 = \text{C18–C23–C24–N(H)},\ \tau 2 = \text{C19–C18–C15–C14},$$

$$\tau 3 = \text{C13–C12–C11–}N,\ \tau 4 = \text{C12–C11–N–C6},$$

$$\tau 5 = \text{C6–N–C5–O}$$

First of all, initial structures were generated by a MD simulation and energy minimization without any constraints. The one with the lowest energy was chosen as the starting structure for an exhaustive systematic search of five dihedral angles ($\tau 1$–$\tau 5$) mentioned above. The final aim was to detect possible bioactive low-energy conformers which would fit the NOE data.

The most rigid part of valsartan is three aromatic rings, which have to take certain orientations to minimize the stereo violations. So the systematic searching started from the dihedral angle $\tau 2$ by rotation around (C–15)–(C–18) bond to define the relative orientation of the biphenyl scaffold. An energy curve with a stepsize of 5° was built in Fig. 3 and two energy minima were picked as S1 and S2 at ±95°. Taking structure S1 or S2 as the starting structure, the orientation of the tetrazole with respect to the terminal phenyl ring was scanned and we found that, calculated from either geometry, the molecule had the lowest energy when $\tau 1 = \pm 30°$.

The dihedral angles $\tau 3$ and $\tau 4$ were scanned simultaneously in the second step of systematic searching starting from the geometry at point S1, because the conformations at point S1 and S2 could interchange from each other by rotating $\tau 3$.

DOI: 10.1002/mrc

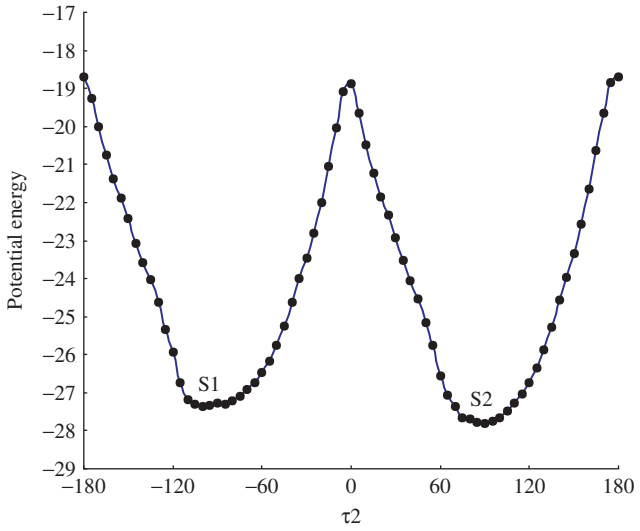

Figure 3. Relative potential energy (kcal mo^{-1}) of valsartan as a function of dihedral angle $\tau 2$, with the unit of Hartree and a stepsize of 5°.

The two-dimensional energy contour plot in Fig. 4 showed several minima on the energy surface, marked in numerical order from S3 to S8. Compared with the NOE patterns we got, only the conformations at point S7 (−60.0, −110.0) and S8 (100.0, −120.0) were consistent with the experimental data and were subjected to the following calculation.

Semi-empirical PM3 method was applied during the first two steps of systematic searching. The last step was carried out using DFT with B3LYP/6-31G* set to draw the energy curve of dihedral angle $\tau 5$ with a stepsize of 30° in Fig. 5. Here structure S7 and S8 served as the starting geometries and the optimized structure of each 30° grid was taken as the initial geometry for the next grid scan. In order to find a strongly stable conformation of valsartan, it is suggested that after 360° scan the structure with the minimal energy is supposed to have the same geometry as the original one; otherwise a second cycle of scan will be performed. Under this rule, the structure scanned from point S7 was considered to be metastable and the final energy curve drawn in Fig. 5 coincided with the one starting from point S8. We got two energy minima with $\tau 5$ located near 0° (I) and 180° (III) and two maxima near 90° (II) and 270° (IV). The geometries of these structures were further optimized without any constraint by an enlarged basis set 6-311G** to improve the accuracy of the energies (Table 5). Thus the barrier of the bond rotation around N–C(O) was 18–20 kcal mo^{-1}, which was in good agreement with our experimental data, 17.9 ± 0.7 kcal mol^{-1}, at 298 K.

The conformations of valsartan at point I and III were illustrated in Fig. 6, showing conserved aromatic part with different orientation of the aliphatic chains. It's clear that the rotation of the N–C(O) bond in valsartan is exactly the *cis/trans* isomerization of the peptide bond observed in peptides and proteins. More interestingly, in both conformations the tetrazole ring was very close to the carboxyl group, with the distances of $d_{N(H)-O} = 0.286$ nm and $d_{N-(H)O} = 0.289$ nm for conformer A and $d_{N(H)-O} = 0.286$ nm and $d_{N-(H)O} = 0.285$ nm for conformer B, which can be easily suspected to be the hydrogen bonds. This explained the conserved dihedral angles that connected the aromatic rings of valsartan. It's important to point out that the tetrazole is a negative charged acidic group in physiological environment and might be crucial to the receptor binding. However, the NMR spectrum was recorded in CD_3OD and to make the

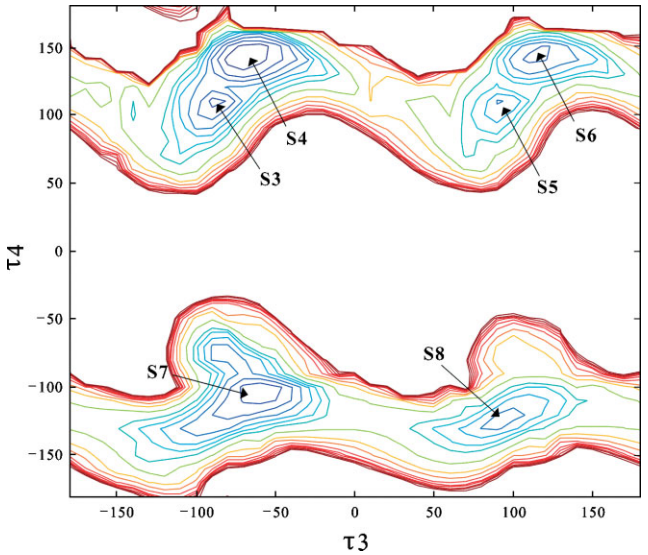

Figure 4. Contour plot of the relative potential energy of valsartan as a function of dihedral angle $\tau 3$ and $\tau 4$, obtained from a system search analysis starting from point S1 in Fig. 3 with a stepsize of 10°.

Table 5. Calculated relative energies (kcal mol^{-1}) and dihedral angles (degree) of the hindered rotation for compound **1** by density functional theory

	I	II	III	IV
ΔE/B3LYP/6-31G(d)	2.59	19.88	0.0	19.07
ΔE/B3LYP/6-311+G(d, p)	2.09	19.83	0.0	18.77
τ_5 (C6-N-C5-O)	1.7	74.8	174.2	289.1

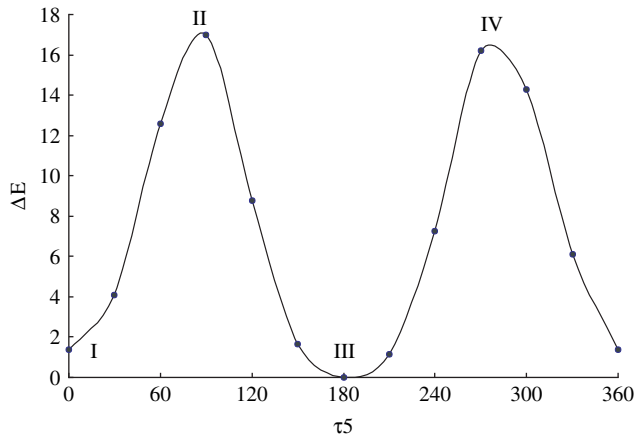

Figure 5. Relative potential energy (kcal mol^{-1}) of valsartan as a function of dihedral angle $\tau 5$ obtained from a system search analysis starting from point S8 in Fig. 4 with a stepsize of 30°.

DOI: 10.1002/mrc

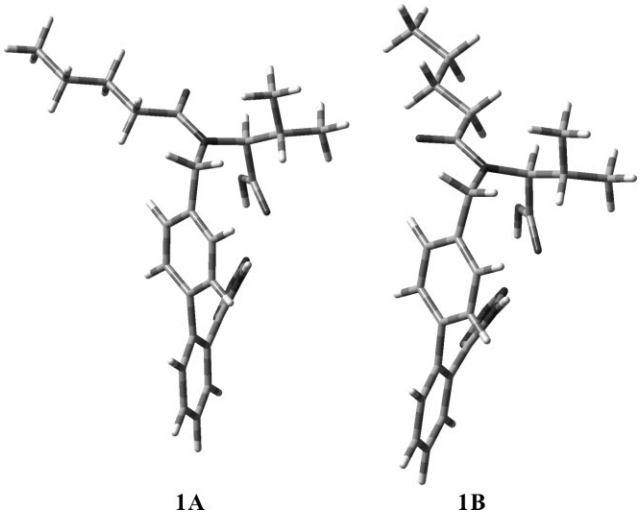

Figure 6. The optimized structures of conformer A and B for valsartan using density functional theory (B3LYP/6-31G*).

calculation system easier, the entire structure calculation was performed in vacuum without the consideration of solvent and charge. So the hydrogen bond may not be true in the solvent when the tetrazole ring is charged.

CONCLUSION

This work describes the application of NMR as a tool for medicinal chemistry in studying valsartan and three related compounds. ^{1}H and ^{13}C NMR resonances of all four compounds were completely assigned using 2D NMR techniques. The exchange rates and thermodynamic parameters of the conformational exchange for compounds **1**, **2,** and **4** were determined by variable temperature NMR experiments, respectively. The conformational analysis of valsartan was performed by a combination of NMR spectroscopy and quantum chemistry calculation showing excellent agreement. The achieved structures showed an intramolecular switch of *cis*/*trans* isomerization of the C(O)–N bond which could be important in the way of its interaction with AT1 receptor binding site. Future studies in our group of protein binding in plasma of valsartan will aid in the elucidation of the mechanism of ligand binding and solving the structures of other valsartan analogs will provide beneficial insight into the design of a broad-spectrum angiotensin II receptor antagonists.

Acknowledgements

This work is supported by the grants from the Natural Science Foundation (#20635040, #20605026, #20610104), and 973 Project of China (2002CB713806).

REFERENCES

1. Bühlmayer P, Furet P, Criscione L, Gasparo M, Whitebread S, Schmidlin T, Lattmann R, Wood J. *Bioorg. Med. Chem. Lett.* 1994; **4**: 29.
2. Noda K, Ideishi M, Tashiro E. *Curr. Ther. Res.* 2003; **64**: 151.
3. Black HR, Cohen JD, Kaplan NM. *Arch. Intern. Med.* 1997; **157**: 2413.
4. Oparil S, Silfani TN, Walker JF. *Am. J. Hypertens.* 2005; **18**: 287.
5. Hillaert S, Bossche WV. *J. Pharm. Biomed.* 2003; **31**: 329.
6. Francotte E, Davatz A, Richert P. *J. Chromatogr. B* 1996; **686**: 77.
7. Maurer HH, Kraemer T, Arlt JW. *Ther. Drug Monit.* 1998; **20**: 706.
8. Şatana E, Altınay Ş, Göder NG, Özkan SA, Şentürk Z. *J. Pharm. Biomed.* 2001; **25**: 1009.
9. Cagigal E, González L, Alonso RM, Jiménez RM. *Talanta* 2001; **54**: 1121.
10. Daneshtalab N, Lewanczuk RZ, Jamali F. *J. Chromatogr. B* 2002; **766**: 345.
11. Verheijen I, Fierens FL, Debacker JP, Vauquelin G, Vanderheyden PM. *Fund. Clin. Pharmacol.* 2000; **146**: 577.
12. Colussi DM, Parisot C, Rossolino ML, Brunner LA, Lefevre GY. *J. Clin. Pharmacol.* 1997; **373**: 214.
13. de Gasparo M, Whitebread S. *Regul. Pept.* 1995; **593**: 303.
14. Bauer M, Harris RK, Rao RC, Apperley DC, Rodger CA. *J. Chem. Soc., Perkin Trans. 2* 1998; **3**: 475.
15. Mavromoustakos T, Kolocouris A, Zervou M, Roumelioti P, Matsoukas J, Weisemann R. *J. Med. Chem.* 1999; **42**: 1714.
16. Yoo SE, Kim SK, Lee SH, Kim NJ, Lee DW. *Bioorg. Med. Chem. Lett.* 2000; **8**: 2311.
17. Zoumpoulakis P, Grdadolnik SG, Matsoukas J, Mavromoustakos T. *J. Pharm. Biomed.* 2002; **28**: 125.
18. Bruch MD. *NMR Spectroscopy Techniques*, Marcel Dekker: New York, 1996.
19. Hore PJ. *Nuclear Magnetic Resonance*, Oxford University Press: Oxford, 1995.
20. Friebolin H. *Basic One- and Two-Dimentional NMR Spectroscopy*, VCH Publishers: New York, 2005.
21. Nie J, Xiang BR, Feng YQ, Wang DH. *J. Liq. Chromatogr. Relat. Technol.* 2006; **29**: 553.
22. Case DA, Darden T, Cheatham TE III, Simmerling CL, Wang J, Duke R, Luo R, Merz KM Jr, Wang B, Pearlman DA, Crowley M, Brozell S, Tsui V, Gohlke H, Mongan J, Hornak V, Cui G, Beroza P, Schafmeister C, Caldwell JW, Ross WS, Kollman PA. *AMBER 8.0*, University of California: San Francisco, 2004.
23. Frisch MJ, Trucks GW, Schlegel HB, Scuseria GE, Robb MA, Cheeseman JR, Montgomery JA Jr, Vreven T, Kudin KN, Burant JC, Millam JM, Iyengar SS, Tomasi J, Barone V, Mennucci B, Cossi M, Scalmani G, Rega N, Petersson GA, Nakatsuji H, Hada M, Ehara M, Toyota K, Fukuda R, Hasegawa J, Ishida M, Nakajima T, Honda Y, Kitao O, Nakai H, Klene M, Li X, Knox JE, Hratchian HP, Cross JB, Bakken V, Adamo C, Jaramillo J, Gomperts R, Stratmann RE, Yazyev O, Austin AJ, Cammi R, Pomelli C, Ochterski JW, Ayala PY, Morokuma K, Voth GA, Salvador P, Dannenberg JJ, Zakrzewski VG, Dapprich S, Daniels AD, Strain MC, Farkas O, Malick DK, Rabuck AD, Raghavachari K, Foresman JB, Ortiz JV, Cui Q, Baboul AG, Clifford S, Cioslowski J, Stefanov BB, Liu G, Liashenko A, Piskorz P, Komaromi I, Martin RL, Fox DJ, Keith T, Al-Laham MA, Peng CY, Nanayakkara A, Challacombe M, Gill PMW, Johnson B, Chen W, Wong MW, Gonzalez C, Pople JA. *Gaussian 03. (B.05)*, Gaussian: Pittsburgh, 2003.
24. Zhao Z, Wang Q, Tsai EW, Qin X-Z, Ip D. *J. Pharm. Biomed.* 1999; **20**: 129.
25. Boyd J, Moore G, Williams G. *J. Magn. Reson.* 1984; **58**: 511.
26. Wynants C, VanBinst G, Mugge C, Jurkschat K, Tzschach A, Pepermans H, Gielen M, Willem R. *Organometallics* 1985; **4**: 1906.
27. Willem R. *Prog. Nucl. Magn. Reson. Spectrosc.* 1987; **20**: 1.
28. Ernst RR, Bodenhausen G, Wokaun A. *Principles of Nuclear Magnetic Resonance in One and Two Dimensions*, Clarendon Press: Oxford, 1992.
29. Evans JNS. *Biomolecular NMR Spectroscopy*, Oxford University Press: Oxford, 1995.